Open Access

SCHOLARENA

Journal of Nanoscience and Nanotechnology Applications

RESEARCH ARTICLE

ISSN: 2577-7920

Exploring of Elastic, Vibrational and Thermoelectric Properties of NaScGe Compound: Ab-initio Study

Ciftci YO*

Department of Physics, Gazi University, Teknikokullar, Ankara, Turkey

***Corresponding author:** Ciftci YO, Department of Physics, Gazi University, Teknikokullar, Ankara, Turkey, Tel.: +90-312-2021266; fax: +90-312-2122279, E-mail: yasemin@gazi.edu.tr

Citation: Ciftci YO (2021) Exploring of Elastic, Vibrational and Thermoelectric Properties of NaScGe Compound: Ab-initio Study. J Nanosci Nanotechnol Appl 5: 101

Abstract

The structural, electronic, elastic, vibrational and thermoelectric features of Half- Heusler semiconductor compound NaScGe with 8 electron valence count which has cubic structure with space group *F*43*m* (No. 216) with regard to the first-principles computations have been investigated. To calculate the thermos-electric properties of NaScGe semi-classical Boltzmann transport theory was considered. The elastic features, like elastic constants, shear modulus, Young's modulus, Poisson ratio, anisotropy factor, Debye temperature and sound velocities were discussed. This compound has been mechanically and dynamically found as stable, according to our calculated elastic and phonon properties. According to the obtained band structure, this compound is a semiconductor which has band gap 1.02 eV. The Seebeck coefficient, electrical conductivity, electronic thermal conductivity, power factor and figure of merit (ZT) as a function of chemical potential and temperature were investigated. NaScGe has a high power factor for p-type doping. The calculated results of ZT parameter (~1) for NaScGe indicate that the investigated material may be used for thermoelectric applications. This Half-Heusler semiconductor compound has been investigated as thermoelectric material for the first time.

Keywords: *ab initio*; Half Heusler; Phonon Frequencies; Thermoelectric

Introduction

The researchers have investigated Heusler and half Heusler compounds due to exhibition of interesting properties [1–7]. Huesler compounds exhibits high spin polarization and high magnetization [8,9]. Because of these properties, these Heusler compounds are favorable for spintronic applications [10-13]. Half- Heusler have technological applications as a spin filter [14], thermoelectric applications [15-19] topological insulators [20]. Half- Heusler compounds are used in electronic devices [21].

In the last decades, the fast consumption rate of available natural sources of energy (oils and gases) due to the large need of mankind demands an alternative source of energy without affecting the environmental conditions [22]. The various devices such as solar, hydro-power, bio-mass and thermoelectric (TE) generators are being used to generate the required electricity. Increasing energy demand leads scientists to look for alternative energy sources. TE materials are one of the energy conversion materials which play a significant role in this area. Even though the research regarding TE materials started decades ago, the limitations in the efficiency of the existing TE materials have made this research an essential topic until today. TE materials can be used to convert waste heat into electricity. By means of this waste heat conversion, this material will help to reduce environmental pollution and this makes this energy source unique.

Mainly, the general applications in thermoelectric devices are restricted in view of their small transformation performance [23]. Generally, the performance of the thermo-electric apparatus can be developed by raising their thermo-electric figure of merit $= \frac{S^2\sigma}{K}T$, where T is the temperature, σ is the electrical conductivity, S is the Seebeck coefficient and K is the thermal conductivity, which is the total of electronic and lattice additions. Thus, materials which have a high Seebeck coefficient, high electrical conductivity and, low thermal conductivity are good TE materials. This can only be obtained in intensely doped semiconductors joining high electron density of states with high mobility and high carrier concentration [24-26].

Half-Heuslers compounds or alloys, low toxicity and future TE properties have attracted great interest from researchers in order to achieve sustainable growth. In addition, half-Heusler materials are also attractive due to their possible potential for medium and

high temperature TE properties [27]. Lately, electronic and thermo-electric properties of half- Heusler compounds XMgN (X=Li, Na, K) have been studied by Ahmad *et al.* [28] using a DFT-based approach in the WIEN2k computational program. For good thermoelectric efficiency the band gap should be range from 0.05- 1.8 eV. Despite the wide band gap range, ZT values have been obtained at a sufficient level for practical applications [28-30] .

The Half- Heusler materials such as MCoSb (M = Ti, Zr, Hf) and MNiSn are paid regard to efficient thermo-electric materials due to better mechanical strength and their low thermal conductivity compared to other available compounds [31,32]. Empirically, in the pure ZrNiSn compound, the maximum dimensionless figure of merit value was observed to be 0.3 at 900K [33].

Using semi-classical Boltzmann transport equations, the first principles method on electronic structure calculations were used to understand the thermo-electric performance of NaScGe. The present study purposes better definition unstudied properties of the structural, elastic, electronic, lattice dynamic and thermoelectric of NaScGe employing the *ab-initio* pseudopotential method.

Computational Method

The structural optimization, electronic, elastic and vibrational properties are performed in the form of density-functional theory using Vienna Ab-initio Simulation Package (VASP) [34-38] within the Perdew-Burke-Ernzerhof [39] shape of the generalized gradient approximation (GGA). To optimize the structure of NaScGe, full relaxation of cell volume, shape and atomic position performed. To obtain high-occuracy results, the total energy and force convergence are set to be 10^{-8} eV and 10^{-6} eV/A, respectively. Plane-wave cut-off energy was taken as 700 eV. The investigated features have been obtained using an 15x15x15 Monckhorst-Pack k mesh, while the electronic properties have been acquired using 42x42x42 Monckhorst-Pack k-point grid. They have been selected as Na($3s^1$) , Sc ($3d^14s^2$) and Ge($4s^24p^2$) for GGA-PBE pseudopotentials for the valence configurations of the component atoms.

Thermoelectric transport coefficients such as Seebeck coefficients (S) , electronic conduction with respect to scattering time (σ/τ) electronic thermal conductivity (ke) using first-principles data have been calculated by resolving Boltzmann transport equations inclusive of the constant relaxation-time (CSTA) and rigid band approximations (RBA) by BOLTZTRAP code [40]. To help obtain correct transport properties, much denser kmesh (42× 42 × 42 in primitive cell) is used to ensure the accuracy of self-consistent energy values. Based on Boltzmann theory, BolttzTraP code calculates transport coefficient depend on various band structures. BoltzTraP code analytically represents these band energies with a smoothed Fourier interpolation and thereafter one can obtain the necessary derivatives such as electron velocities for transport properties.

To investigate the vibration properties, the dispersion relation due to phonons have been investigated using PHONOPY package [41] after obtaining harmonic 2nd order interatomic force constants (IFCs) in the form of harmonic approximation and supercell approach. The IFCs are obtained using method based supercell upon density functional perturbation theory (DFPT) as implemented in VASP package. To obtain the phonon dispersion relations of NaScGe, we perform 2 × 2 × 2 supercell including 24 atoms and 0.01 Å atomic displacement distance to calculate the second-order force constants by using VASP code. For Brillouin zone integration, we used 8 × 8 × 8 k-mesh and 700 eV cutoff criteria for plane wave basis set.

The elastic constants were obtained after performing energy-strain calculations with the applications of little strain to an optimized unit cell. This method is used to calculated the second derivative of the total energy with respect to the strain.

Results and Discussion

Structural properties and electronic band structure

NaScGe crystallizes in the cubic MgAgAs-type structure with a *F*43*m* space group where Na, Sc and Ge occupy the sites (0.5; 0.5; 0.5), (0,0,0) and (0.25; 0.25; 0.25), respectively, as given in Figure 1.The structural properties of NaScGe are obtained using energy minimization method. In our calculations, both k-point sampling and the kinetic energy cutoff have been carefully checked for the eneough accuracy. The fully relaxed equilibrium structure have been obtained by minimizing the total energy. To optimize structural parameterr such as atomic positions and lattice parameters, forces and stress tensors were minimized. To determine the equilibrium geometry, the all atomic positions and the volume of unit cell have been relaxed. The volume- energy curve which is fitted by the Murnaghan's equation of state [42] is given in Figure 2. The obtained lattice constant (a), bulk modulus (B), derivative of bulk modulus (B') for NaScGe are given in Table 1. There is no experimental data to compare our results to the best of our knowledge. But, our calculated lattice constant is good agreement with the other calculations in Ref. [43]. As well- known that the GGA gives mildly overestimated lattice constants for the experimental data. The obtained results are given in Table 1. The obtained B and B' are given as 44.59 GPa and 4.08 for NaScGe (Table 1). Unfortunately, to our knowledge, for the bulk modulus and its pressure derivative, there are no former data in the literature for the check.

Material	Reference	a (Å)	B (GPa)	B'	Eg(eV)
NaScGe	Present	6.643	44.59	4.08	1.02
Theory[a]		6.645			0.681(GGA)

Table 1: Equilibrium lattice constants *(a)* bulk modulus *(B)*, pressure derivative of bulk modulus *(B')* and band gap (Eg) for NaScGe, together with other theoretical results a: [43]

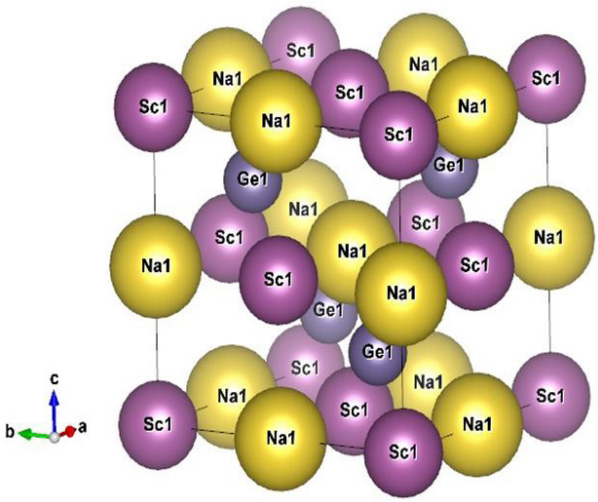

Figure 1: Crystal structure of NaScGe

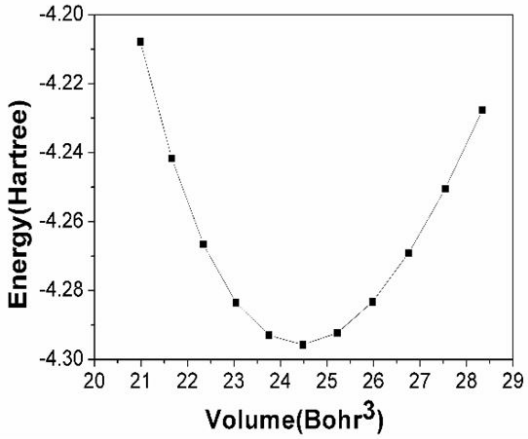

Figure 2: Energy-volume curves for NaScGe

The chemical composition, crystal structure, and band structure of materials is important for the transport coefficient of thermoelectric semiconductor materials. Our obtained electronic band structure graph is given in Figure 3. The Fermi level is arranged to be 0 eV. Due to the fact that both the valence band maximum (VBM) and conduction band minimum (CBM) is constituted at the Γ point, the calculated band structure of NaScGe exhibits direct band gap. Our obtained the energy band gap value *Eg* of 1.02 eV is in good agreement with the 1.04 eV [43]. This difference is result in from the exchange-correlation approximation of DFT. It can be seen from electronic band structures that there exists a association of heavy and lightweight bands near the VBM, for the valence band maximum (VBM) is located at the Γ point, and the dispersion along the Γ-X direction is greater than the Γ- L direction.

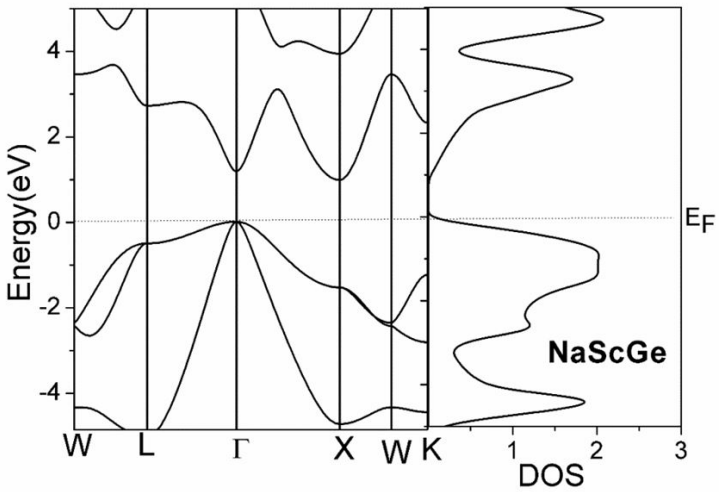

Figure 3: Electronic band structure of NaScGe along different symmetry directions

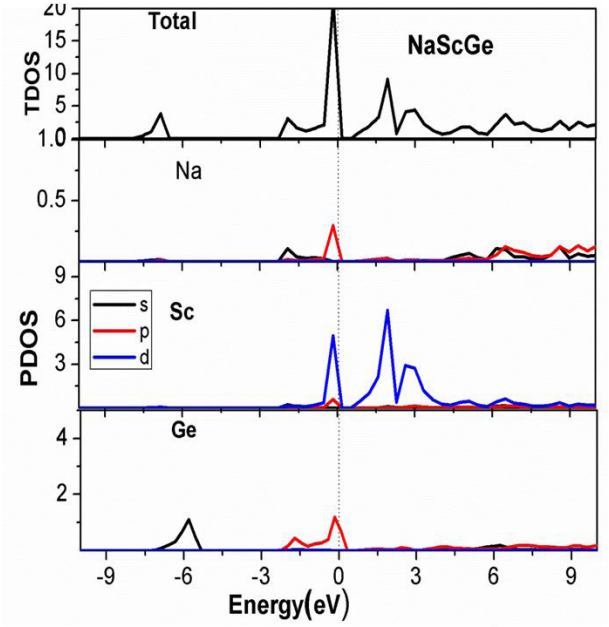

Figure 4: Total and atom-projected density of states of NaScGe

Moreover, the contributions of various atoms for the evolution of band structure can be appeared by the total DOS. However, the partial DOS information may be even more helpful in understanding the details of certain contributions of various atomic states. The total and partial density of states (DOS) which is used for, how distinct atoms and their local coordination, command the energy band structure of NaScGe are given in Figure 4 to understand. The contribution in DOS between -8 and -5 eV in the lower valance band region, is mainly due to 4-s-state of Ge. In the upper valance band region from 0 to -2.8eV in the valence band, the energy bands are chiefly determined by Sc-3d states while p-orbitals of Na and Sc Pb show minor contribution. From the PDOS graphs, it is seen that Sc-3d orbitals contribute more in the both valence and conduction band. Therefore, it can be concluded that the Sc 3d-orbitals are important to decide the thermoelectric properties of NaScGe. The sharp band in valance band indicates that this compound has a high power factor in p-type compound.

L- Γ (heavy hole) m_{hh}	0.872
L- Γ (light hole) m_{lh}	0.025
Γ- X (heavy hole) m_{hh}	0.110
Γ- X (light hole) m_{lh}	0.031
Γ- X (electron) m_e	0.065
X-W (electron) m_e	0.019

Table 2: Effective masses of the electrons (me) and holes (mh) at different symmetry points of the irreducible Brillouin zone

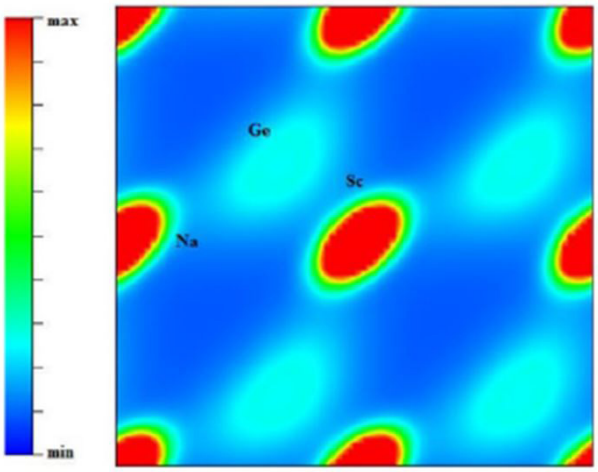

Figure 5: Calculated electron density map in direction [100] for NaScGe

One of the important factors specifying the transport properties of the materials is the effective mass of the charge carriers. Generally, the lower / higher effective mass means the migration capacity of the carriers in the semiconductor materials and the higher / lower the probability of low / high recombination chance of carriers within semiconductor materials. Since the effective mass exhibits a direct connection with the thermopower and an inverse connection with the electrical conductivity, investigation of the effective mass (m*) of the charge carriers has a conflict. The higher the value of m* gives a higher thermopower but lower electrical conductivity. As a result, the high effective mass is a sign of good thermoelectric efficiency. It is seen from table 2 that at the conduction band minimum the effective mass of electron is smaller than that of the hole at the valence band maximum. Finally, the *p*-type NaScGe may have the highest Seebeck coefficient.

The charge density map gives the nature of chemical bonding. The calculated electron densities of NaScGe in direction [100] are shown in Figure 5. While electronegativity of crystal-forming elements determine the nature of binding between atomic components, a major difference in electronegativity plays a major role in causing a charge transfer between different atoms, thus leading to an ionic bond quality. On the contrary, the small difference in electronegativity leads to charge sharing, which is in charge of covalent bond the nature [44]. In this map, the lighter areas show electron loss while the darker region exhibits electron gain. The electron profit on Na is greater than on the Sc and Ge. It can be seen Figure 5 that the charge density disperse has spherical form, showing that the bonding is generally ionic for NaScGe.

Elastic Properties

The elastic constants are described by the reaction of a solid under external forces. By using calculated the elastic feature like shear, bulk, and Young's moduli and Poisson's ratio, the stability of a material can be determined. The "stress-strain" method [45,46] is employed to calculate the second-order elastic constants (C_{ij}). The obtained second-order elastic constants and bulk modulus are tabulated in Table 2. The Born stability conditions, which must be satisfied for the stability of the lattice, are tested using second order elastic constants [47]. For cubic crystals, the mechanical stability conditions are determined with regard to Born's stability criteria:

$$C_{11}>0,\ C_{11}-C_{12}>0,\ C_{44}>0,\ C_{11}+2C_{12}>0 \text{ and } C_{12}<B<C_{11}.$$

According to this criteria, a NaScGe compound in MgAgAs structure is mechanically stable. According to our information in literature, there are not available experimental and theoretical data on the elastic properties for NaScGe. As a result, it can be concluded that the given calculated elastic constants may add valuable data to available literature.

Using the calculated elastic constants, it can be determined different elastic properties, like Shear modulus ($G = (C_{11}-C_{12}+2C_{44})/4$), Young's modulus ($E$) and Poisson ratio ($v$), Zener anisotropy factor (A). Also, these properties define the strength of a material as is seen in Table 3. High shear modulus shows covalent nature [48,49]. As it can be seen from Table 3, NaScGe exhibits soft material due to the low Young's and shear moduli. To estimate ductility, it can be used a correlation of bulk / shear moduli (G/B) proposed by Pugh [50]. The bulk modulus B represents the resistance to fracture while the shear modulus G demonstrates the resistance to plastic deformation. If the G/B relation is smaller/greater than 0.57, the material indicates the ductile/brittle behavior. As seen from Table 3, according to G/B ratio of 0.47 for NaScGe, this compound has ductile nature.

The degree of directivity of covalent bonds is reflected by Poisson's ratio. For estimating the ductility, poisson's ratio can be used. Generally, poisson's ratio is higher than 0.33 for ductile compounds [51]. In solid, for central forces and ionic crystals, the lower limit and upper limit of υ are given as 0.25 and 0.5, respectively [52]. Besides, for covalent materials and non-central forces, these values are given between 0.1 and 0.25 [53]. Herein, the calculated υ value for NaScGe is 0.297. It can be concluded from Table 2 that NaScGe has ionic bonding and the interatomic forces are central.

The Zener anisotropy factor (A) is a test of the rating of elastic anisotropy in solids. A is equal to 1 for isotropic crystals, but the values smaller or greater than 1 show the scale of elastic anisotropy [49]. For this compound the calculated Zener anisotropy factor is 0.620, which shows that NaScGe is definitely anisotropic material.

C_{11} (GPa)	C_{12} (GPa)	C_{44} (GPa)	G (GPa)	E (GPa)	υ	G/B	Θ (K)	A	V_l (m/s)	V_t (m/s)	V_m (m/s)
82.7	26.7	17.5	21.1	54.7	0.297	0.47	294.9	0.62	4795	2574	2874

Table 3: Elastic constants C_{ij} (GPa), Young Modulus E (GPa), shear modulus G (GPa), poisson's ratio (υ), G/B ratio, Zener Anisotropy factor (A), Debye temperature θ (K) and sound velocities $v_p v_t v_m$ (m/s) for NaScGe

The Debye temperature with regard to a lot of physical features such as specific heat and melting temperature is a significant basic parameter nearly. At low temperatures, the vibration stimulus occur merely with acoustic vibrations. Therefore, the Debye temperature θ_D at low temperatures obtained from elastic constants is the same as that specified from specific heat evaluation. The Debye temperature, θ_D, obtained from the elastic constant data employing the mean velocity, v_m, are calculated by the below relation [54]:

$$\theta_D = \frac{h}{k}\left[\frac{3n}{4\pi}\left(\frac{N_A\rho}{M}\right)\right]^{13} \upsilon_m \quad (1)$$

here k is Boltzmann's constants, h is Planck's constants, n is the number of atoms per formula unit, N_A is Avogadro's number, M is the molecular mass per formula unit, ($\rho = M/V$) is the density, and vm is obtained from [55]

$$\upsilon_m = \left[\frac{1}{3}\left(\frac{2}{\upsilon_t^3}+\frac{1}{\upsilon_l^3}\right)\right]^{-13} \tag{2}$$

Here v_l and v_t, which are calculated from Navier's equations, are the longitudinal and transverse elastic wave velocities, respectively [48]:

$$\upsilon_l = \sqrt{\frac{3B+4G}{3\rho}} \tag{3}$$

and

$$\upsilon_t = \sqrt{\frac{G}{\rho}} \tag{4}$$

The obtained average, longitudinal and transverse elastic wave velocities, Debye temperature for NaScGe are given in Table 2. Unfortunately, there are no data given in the literature for the comparison.

As regards an empirical rule, materials which are a high Debye temperature, high melting point and large thermal conductivity have high values of B and G. The relatively low Debye temperature will result in little Hall mobility and low thermal conductivity [56]. The calculated B (44.59 GPa) and G (21.1 GPa) values are less than the well-known high temperature half Heusler compound NbFeSb (163.2 and 79 GPa)[57] and Ru based half Heusler compounds [58] indicating that NaScGe has a small value of melting point and lattice thermal conductivity as compared with half Heusler compounds.

For small sound velocity, materials which have soft lattices and little elastic constants, the lattice thermal conductivity κ_{latt} is smaller, and phonon dispersion curves ordinarily give low laining optical phonon modes [59]. In this stuation, it is concluded the anharmonic coupling between these optical phonon and acoustic phonons and for this reason, this effect induces a strong scattering of acoustic phonon [59, 60]. From Table 2, it can be seen that investigated compound has an elastic anisotropic in nature. The sound velocity which is closely related to the thermal conductivity in material is determined by deploying direction and through the crystal symmetry [61]. High values of sound velocities for NaScGe are indicated that this compound can be used in production of high-temperature acoustical apparatus.

Phonon Dispersion Curves

The lattice dynamical stability becomes more prominent properties of the material under zero pressure and finite pressure. Thus, the phonon frequencies of the cubic MgAgAs phase of NaScGe have been obtained the PHONOPY code [41], which is referring the forces gotten from the VASP. Employing the density functional perturbation theory, The PHONOPY code obtains force constant matrices and phonon frequencies [41]. The obtained phonon dispersion graph along several high symmetry directions using a 2x2x2 supercell of 24 atoms was given in Figure 6. Unlikely, there are no available experimental and other theoretical study for comparing the lattice dynamics for the investigated compound. The phonon graph has 9 phonon branches, involving three acoustic branches and 6 optical branches for NaScGe compound which has 3 atoms in the primitive cell. It can be seen from Figure 6 that none of the branches involve a negative frequencies in the whole Brillouin zone (Figure 6). Thus, this graph strongly stands for the dynamical consistency of NaScGe compound in MgAgAs structure. As you can see on the right side of Figure 6, the phonon spectrum of the NaScGe compound involves three groups of bands. The lower modes with frequencies up to 3.0 THz are mainly defined by the vibrations of the Ge atoms. The modes in the range 3-5.5 THz are defined by the vibrations of the Ge and Sc atoms, while the vibrations of the Na atoms, which are heavy, are in the upper range of 6-7.5 THz. As seen from Figure 6 that there is low-frequency optic branches that intersect the acoustic branches starting well below 4 THz. This result shows strong phonon-phonon scattering, indicating low thermal conductivity. From Figure 6, it can be seen that these lower frequency modes result from generally due to the vibrations of Ge atoms.

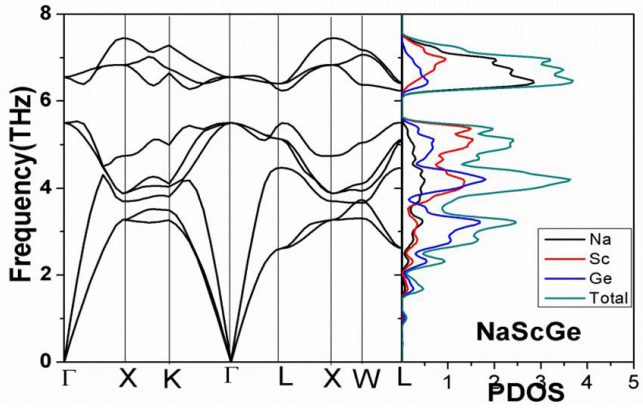

Figure 6: Phonon dispersion curves for NaScGe

Transport properties

In Figure 7, the change of Seebeck coefficient in temperature and concentration are given for this material. The Seebeck coefficient is a significant means of testing of the electronic structures of the materials near the Fermi energy. The bigger values of Seebeck coefficient are desirable for productive TE apparatus. For this material, the maximum Seebeck coefficient value is found for p- type doping and the optimum carrier concentration is obtained as 10^{17} cm^3. At 10^{17} cm^3 carrier concentrations, the obtained Seebeck coefficient (S), electrical conductivity (σ/τ), electronic thermal conductivity (ke/τ) and power factor ($S^2\sigma/\tau$) of NaScGe are described in Figures 8,9,10 and 11 as function of chemical potential.

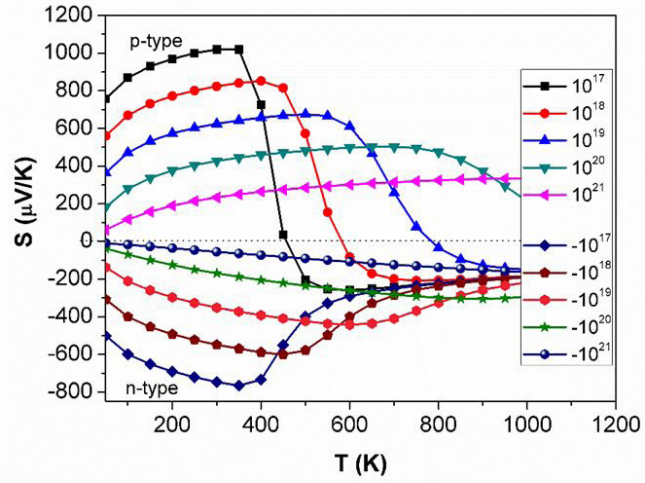

Figure 7: Variation of Seebeck coefficient NaScGe at different concentration (cm^3) and temperature

Seebeck coefficient (S) stand on the electronic properties of the compounds is one of the important parameters. At different temperatures, the variation of Seebeck coefficient as a function of the chemical potentials for NaScGe compound is given in Figure 8. It can be seen from Figure 8 that at room temperature the Seebeck coefficient is a greater than value as that of 600 and 900 K. The biggest value of S for the *p-type* regions is 1212 μV/K for this compound, while the maximum values of S is acquired at 1000 μV/K for the *n-type* doping. The power factor (PF) is equal to the Seebeck coefficient square times and electrical conductivity, which is an important property in examining the efficiency of thermoelectric material. For NaScGe, the obtained power factor increases with residual temperature. In the environs of Fermi level, the power factor shows the minimum and beyond, the power factor rises quickly to form two notable peaks for p-/n-type of the this material.

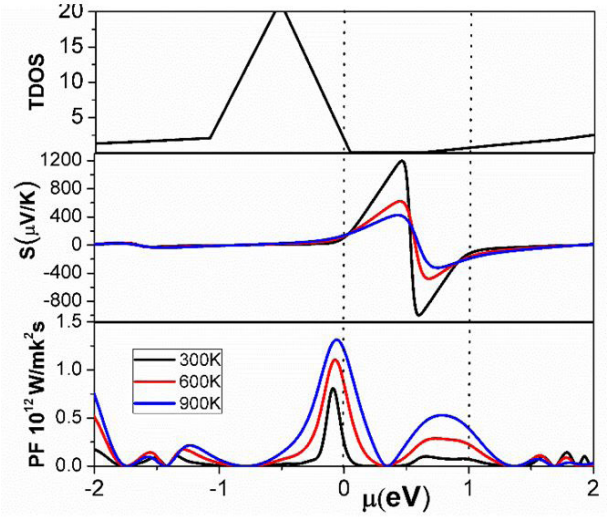

Figure 8: Density of states ,Seebeck coefficients, and power factors of NaScGe towards chemical potentials at 300, 600 and 900 K

At an optimum value of 1.0 x 10^{17} cm^3 carrier concentrations, a function of temperature, the obtained electrical conductivity (σ), Seebeck coefficient (S), electronic thermal conductivity (ke) have been given in Figure 9(a-d). The width of band gap and the sharp density of states near the Fermi level are good mark of the thermoelectric properties of materials. Band structure of NaScGe, has a flat valence band and a sharp conduction band which confirms that this compound may have good transport properties.

It is obvious from Figure 9(a) that the Seebeck coefficient is highly variable with temperature for NaScGe. The Seebeck coefficient values of NaScGe begin from 756 (μV/K) and rises exponentially for this compound, due to the rise in temperature up to 350K and then at higher temperature shows merely constant rate. At 350 K, for this compound, the maximum values of Seebeck coefficient is 1022 μV/K which verified that the investigated material has latent applications in thermoelectric apparatus. The change of electrical conductivity is given in Figure 9(b), per relaxation time of NaScGe with temperature. It can be seen obviously from Figure 9(b) that the electrical conductivity almost exponentially increases with temperature up to 1000K as also seen Figure 9(c) for thermal conductivity. At 1000K, the highest obtained value for electrical conductivity for this compound is 1299×10^{15} $(\Omega.m.s)^{-1}$. ZT_e as a function of T curve is shown in Figure 12(d). The ZT increases from 0.75 to 1.0 which is enough for practical applications as the temperature increases from 50 to 350 K. After 350 K, ZT_e decreases till 0.001 at 450K, then increase up to 0.15 at 1000K .

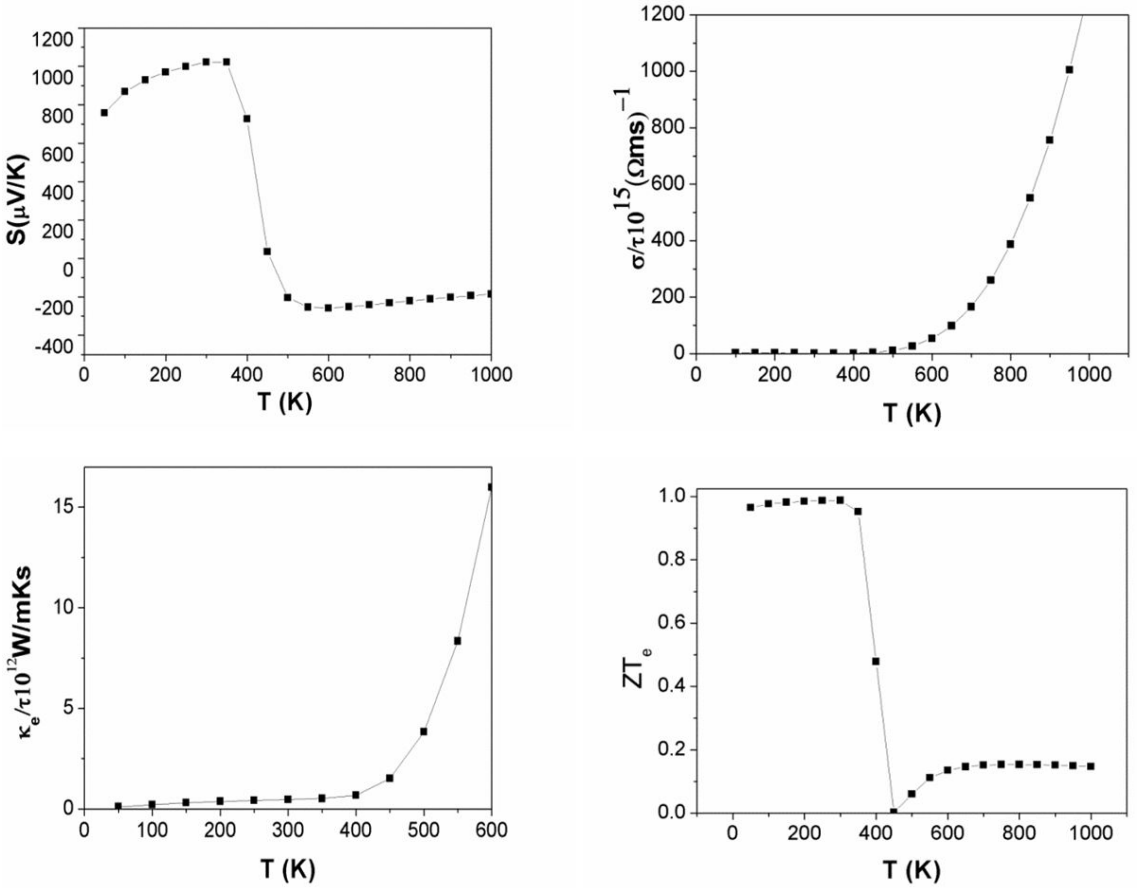

Figure 9: The calculated Seebeck coefficient, electrical conductivity (in unit of relaxation time τ), thermal conductivity (in unit of relaxation time τ) and Figure of merit ZT_{el} as a function of temperature for NaScGe

The Gruneisen parameter (γ) [62] has been calculated depending on Poison's ratio (ν) as follows,

$$\gamma = \frac{3(1+\nu)}{2(2-3\nu)} \tag{5}$$

The γ value for NaScGe has been found to be 1.87, which is greater than those for a well-known TE compound PbTe (1.45) [63] with a low K of 2.4 W/mK at 300 K, RuNbSb (1.74), and RuVSb (1.81) [64]. This higher γ points out a stronger anharmonic scattering of phonons. The Slack equation [65] gives the lattice thermal conductivity as below:

$$K_l = A\frac{\bar{M}\theta_D^3\delta}{\gamma^2 T n^{2/3}}, \tag{6}$$

where $\bar{M}$ denotes the average atomic weight, T is the absolute temperature while θ_D refers to Debye temperature, and in the unit cell, δ is the cube roof of the average volume per atom and n is the number of atoms. A is a coefficient as a function of γ [66] and defined by the following equation,

$$A(\gamma) = \frac{5.720 \times 0.849 \times 10^7}{\left[1 - \left(\frac{0.514}{\gamma}\right) + \left(\frac{0.228}{\gamma^2}\right)\right]}. \tag{7}$$

The graph of K versus temperature for NaScGe has been shown in Figure 10 and at the room temperature K value has been evaluated as 4.91 W/mK. It is lower than that of FeNbSb (22.8 W/mK) which is a novel promising p-type half-Heusler TE material [64].

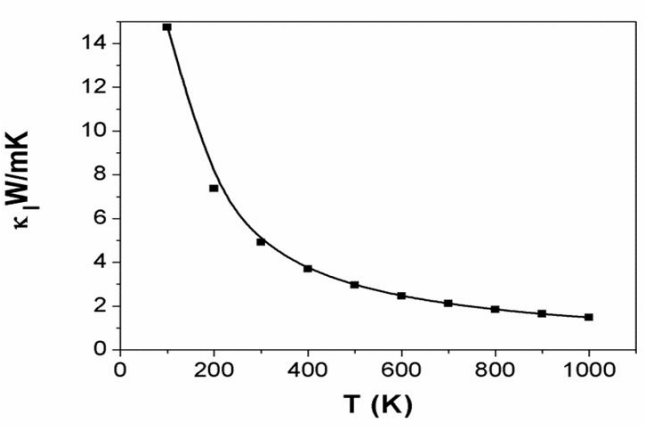

Figure 10: The calculated lattice thermal conductivity as a function of temperature for NaScGe

Conclusions

In this study, the structural, elastic, electronic, vibrational and thermoelectric properties of the Half- Heusler compound NaScGe have been investigated density functional theory(DFT) method and semi classical Boltzmann theory. The obtained lattice constant is good agreement with the theoretical value. Calculations of the electronic structure show that NaScGe is direct band-gap semiconductors. The elastic results reveal that this compound is elastically stable with ductile nature. Besides, the positive phonon frequencies imply is dynamically stable of the MgAgAs structure of this compound. In relation to energy band, the thermoelectric properties have been computed. The optimized carrier concentration is calculated to be the value of 1×10^{17} cm^{-3}. A obtained results for NaScGe are indicated that this compound is a possible new thermoelectric material with a small lattice thermal conductivity, 4.91 W/mK at room temperature. The maximum value of ZT_e at 300 K is 1.0. Our theoretical results may ensure a fine reference data to experimentalists to design this compound for thermoelectric applications. As a result, it can be concluded that the investigated material is encouraging applicant for thermoelectric applications.

References

1. RA deGroot, FM Mueller, PG vanEngen, KHJ Buschow (1983) New Class of Materials: Half-Metallic Ferromagnets Phys Rev Lett 50: 2024.

2. S Chadov, X Qi, J Kubler, GH Fecher, C Felser, (2010) Tunable multifunctional topological insulators in ternary Heusler compounds. Nat Mater 9: 541-5.

3. H Lin, A Wray, Y Xia, S Xu, S Jiaa, A et al (2010) Half-Heusler ternary compounds as new multifunctional experimental platforms for topological quantum phenomena. Nat Mater 9: 546.

4. C Felser, GH Fecher, B Balke (2007) Spintronics: a challenge for materials science and solid-state chemistry Angew Chem Int Ed 46: 668.

5. Q Shen, L Chen, T Goto, T Hirai, J Yang, et al (2001) Effects of partial substitution of Ni by Pd on the thermoelectric properties of ZrNiSn-based half-Heusler compounds. Uher Appl Phys Lett 79: 4165.

6. GS Nolas, J Poon, MG Kanatzidis (2006) Recent Developments in Bulk Thermoelectric Materials. Mat Resaerch Bull 31: 199-205.

7. B Balke, J Barth, M Schwall, GH Fecher, C Felser (2011) An Alternative Approach to Improve the Thermoelectric Properties of Half-Heusler Compound. J Electron Mater 40: 702.

8. J Kubler, GH Fecher, C Felse (2007) Understanding the trend in the Curie temperatures of Co2-based Heusler compounds: Ab initio calculations. Phys Rev B 76: 024414.

9. HC Kandpal, GH Fecher, C Felse (2006) Correlation in the transition-metal-based Heusler compounds Co2 MnSi and Co2 FeSi. Phys Rev B 73: 094422.

10. BT Jonker, YD Park, BR Bennett, HD Cheong, G Kioseoglou, et al. (2000) Phys Rev B 62: 8180.

11. J Schliemann, JC Egues, D Loss (2003) Nonballistic Spin-Field-Effect Transistor. Phys Rev Lett 90: 146801.

12. XH Lou, C Adelmann, SA Crooker, ES Garlid, J Zhang, et al. (2007) Electrical detection of spin transport in lateral ferromagnet–semiconductor devices Nat Phys 3: 197.

13. T Miyazaki, S Kumagai, T Yaoi (1997) Spin tunneling in Ni–Fe/Al2O3/Co junction devices (invited). J Appl Phys 81: 3753.

14. KA Kilian, RH Victora (2000) Electronic structure of Ni2MnIn for use in spin injection. J Appl Phys 87: 7064.

15. P Larson, SD Mahanti, S Sportouch, MG Kanatzidis (1999) Electronic structure of rare-earth nickel pnictides:Narrow-gap thermoelectric materials. Phys Rev B 59: 15660.

16. C Uher, J Yang, S Hu, DT Morelli, GP Meisner (1999) Transport properties of pure and doped MNiSn (M=Zr, Hf). Phys Rev B 59: 8615.

17. DP Young, P Khalifah, RJ Cava, AP Ramirez (2000) Thermoelectric properties of pure and doped FeMSb (M=V,Nb). J Appl Phys 87: 317.

18. Y Xia, V Ponnambalam, S Bhattacharya, AL Pope, SJ Poon, et al. (2001) Electrical transport properties of TiCoSb half-Heusler phases that exhibit high resistivity. J Phys Condens. Matter 13: 77.

19. P Hermet, K Niedziolka, P Jund (2013) A first-principles investigation of the thermodynamic and mechanical properties of Ni–Ti–Sn Heusler and half-Heusler materials. RSC Adv 3: 22176.

20. W Feng, Di Xiao,Ying Zhang, Yugui Yao (2010) Half-Heusler topological insulators: A first-principles study with the Tran-Blaha modified Becke-Johnson density functional . arXiv:1010.2179.

21. KEHM Hanssen, PE Mignarends (1986) Positron-annihilation study of the half-metallic ferromagnet NiMnSb: Theory. Phys Rev B 34: 5009.

22. FJ Di Salvo (1999) Thermoelectric Cooling and Power Generation. Science 285: 703-6.

23. M Cutler, JF Leavy and RL Fitzpatrick (1964) Electronic Transport in Semimetallic Cerium Sulfide . Phys Rev 133: A1143–52.

24. G Slack (1995) in CRC Handbook of Thermoelectrics, edited by D. M. Rowe ,CRC Press, Boca Raton : 407-40.

25. ES Toberer, A Zevalkink, N Crisosto, and GJ Snyder (2010) The Zintl Compound Ca5Al2Sb6 for Low-Cost Thermoelectric Power Generation. Adv Funct Mater 20: 4375.

26. ES Toberer, CA Cox, SR Brown, T Ikeda, AF May, et al. (2008) Traversing the Metal-Insulator Transition in a Zintl Phase: Rational Enhancement of Thermoelectric Efficiency in Yb14Mn1–xAlxSb11 . Adv Funct Mater 18: 2795.

27. G Melnyk (2000) Thermoelectric properties of ternary transition metal antimonides. J Alloys Compd 296: 235–42.

28. R Ahmed, NS Masuri, B Ul Haq, A Shaaria, S AlFaific, et al. (2017) Synthesis and characterization of economical, multi-functional porous ceramics based on abundant aluminosilicates. Materials and Design 136: 196–203

29. I Khan, S Hussaın, J Mınar, S Azam (2018) J of elec Mat 47: 1131

30. Min-Ling Liu, Fu-Qiang Huang, Li-Dong Chen, and I-Wei Chen (2012) Applıed Physıcs Lletters 94: 202103.

31. SR Culp, JW Simonson, SJ POON, V Ponnambalam (2008) (Zr,Hf)Co(Sb,Sn) halfHeusler phases as high-temperature (> 700 °C) p-type thermoelectric materials. Appl Phys Lett 93.

32. LL Wang, L Miao, ZY Wang, W Wei, ZY Xiong, et al. (2009) Thermoelectric performance of half-Heusler compounds TiNiSn and TiCoSb. J Appl Phys 105: 013709.

33. H Muta, T Yamaguchi, K Kurosaki, S Yamanaka (2005) Thermoelectric properties of ZrNiSn based half Heusler compounds, in: Proceedings of the 24th International Conference on Thermoelectrics (ICT 2005).

34. G Kresse and J Hafner (1993) Phys Rev B 47: 558.

35. G Kresse and J Furthmüller (1996) Phys Rev 54: 11169.

36. RM Martin (2004) Electronic Structure , Cambridge University Press, Cambridge, England.

37. PE Blöchl (1994) Projector augmented-wave method. Phys Rev B 50: 17953.

38. G Kresse and D Joubert (1999) From ultrasoft pseudopotentials to the projector augmented-wave method. Phys Rev B 59: 1758.

39. JP Perdew, K Burke, M Ernzerhof (1996) Phys Rev Lett 77: 3865.

40. GKH Madsen and DJ Singh (2006) BoltzTraP. A code for calculating band-structure dependent quantities. Comput Phys Commun 175: 67.

41. A Toga, F Oba and I Tanaka (2008) First-principles calculations of the ferroelastic transition between rutile-type and CaCl2-type SiO2 at high pressures. Phys Rev B 78: 134106-9.

42. FD Murnaghan (1944) The compressibility of media under extreme pressures. Proc Natl Acad Sci 30: 244–7.

43. S Kacimi, H Mehnane, A Zaoui (2014) J.of Alloys Comp 587: 451

44. HU Din, G Murtaza, T Ouahrani, R Khenata, Naeemullah SB (2014) J Alloys Compd 617: 575

45. L Page and P Saxe (2002) Phys Rev B 65: 104104.

46. MJ Mehl, JE Osburn, DA (1990) Papaconstantopoulos, and B. M. Klein (1990) Phys Rev B 41: 10311–23.

47. M Born and K Huang (1956) Dynamical Theory of Crystal Lattices, Clarendon Press.

48. B Mayer, H Anton, E Bott, M Methfessel (2003) Schmidt Intermetallics 11: 23.

49. M Evecen, YO Ciftci (2017) J Nanoelectron Optoelectron 12: 100.

50. SF Pugh (1954) XCII. Relations between the elastic moduli and the plastic properties of polycrystalline pure metals. Philos Mag 45: 823.

51. B Fatima, SS Chouhan, N Acharya. SP Sanyal (2014) Intermetallics 53: 129.

52. HZ Fu, DH Li, F Peng, T Gao and XL Cheng (2008) Comput Mater Sci 44: 774.

53. J Haines, JM Leger, G Bocquillon (2001) Ann Rev Mater Res 31: 1.

54. I Johnston, G Keeler, R Rollins, S Spicklemire (1996) Solids State Physics Simulations, the Consortium for Upperlevel Physics Software, Wiley, New York.

55. OL Anderson (1963) J Phys Chem Solids 24: 909.

56. Xue L, Xu B, Zhao D G and Yi L (2014) Intermetallics 55: 204.

57. AJ Hong, L Li, R He, JJ Gong, ZB Yan, (2016) Original Articles Full-scale computation for all the thermoelectric property parameters of half-Heusler compounds. Ren Sci Rep 6: 22778.

58. T Fang, S Zheng, T Zhou, L Yan, and P Zhang (2017) Phys Chem Phys 19: 4411.

59. G Yumnam, T Pandey and AK Singh (2015) High temperature thermoelectric properties of Zr and Hf based transition metal dichalcogenides: A first principles study. J Chem Phys 143: 234704.

60. L Zhang, MH Du, and DJ Singh (2010) Electronic structure and thermoelectric properties: PbBi2Te4 and related intergrowth compounds. Phys Rev B 81: 075117.

61. M Holland (1963) Phys Rev B 132: 2461.

62. C Kittel (2004) Introduction to Solid State Physics, eighth ed., John Wiley&Sons, Hoboken, USA: 156.

63. DT Morelli and GA Slack (2006) High Lattice Thermal Conductivity Solids, in: S. L. Shindé and J. S. Goela (eds.), High Thermal Conductivity Materials, first ed., Springer, New York, USA.

64. T Fang, S Zheng, T Zhou, L Yan, (2017) Computational Prediction of High Thermoelectric Performance in p-type Half-Heusler Compounds with Low Band Effective Mass, Phys. Chem. Chem Phys 19: 4411-7.

65. VN Belomestnykh and EP Tesleva (2004) Interrelation between Anharmonicity and Lateral Strain in Quasi-Isotropic Polycrystalline Solids. Tech Phys 49: 1098-1100.

66. CL Julian (1965) Theory of Heat Conduction in Rare-Gas Crystals. Phys Rev 137 A128-137.